Paclitaxel and Radiotherapy: Sequence-dependent Efficacy—A Preclinical Model[1]

Alessandra Niero, Ermanno Emiliani, Giuseppe Monti, Flavio Pironi, Livia Turci, Anna Maria Valenti, and Maurizio Marangolo[2]

Dipartimento di Oncologia [A. N., E. E., L. T., M. M.] and Dipartimento di Patologia Clinica [G. M., F. P., A. M. V.], Ospedale S. Maria delle Croci, 48100 Ravenna, Italy

ABSTRACT

The optimal sequence of a paclitaxel-radiation combination was investigated *in vitro* in two human colon adenocarcinoma cell lines, HT29 and LoVo. Three schedules of combined treatment were tested by clonogenic and flow cytometric assays. Paclitaxel was given 24 h prior to a single radiation shot (first schedule) or 24 h (second schedule) or 48 h (third schedule) before 3 days of concomitant radiation. Dose-response data were fit to a linear quadratic model, and mean inactivation dose and sensitizer enhanced ratio were calculated. In HT29 cells, the first and second schedule resulted in an additive effect, whereas a supraadditive interaction was observed with the third combination schedule. This effect was obtained with amounts of paclitaxel lower than IC_{50}, which did not result in cell cycle perturbation, and with low radiation dose (2 Gy) that may be given in a clinical setting. LoVo cells were less sensitive to combined treatment than HT29 cells, switching from infraadditive (first and second schedule) to additive interaction (third schedule). Post-treatment recovery studies of third schedule showed a loss of cell survival in HT29 cells but not in LoVo cells. In contrast to LoVo cells, the third schedule in HT29 cells was able to induce perturbation of cell cycle kinetics, an effective impairment of DNA repair, and apoptotic cell death. HT29 and LoVo cells showed constitutional different characteristics: HT29 cells were more sensitive to paclitaxel exposure, less radiosensitive, and had a different cell cycle redistribution after radiation exposure than LoVo cells; moreover, HT29 cells showed a major propensity to undergo apoptosis. These results suggest that the radiosensitizing effect of paclitaxel was strictly schedule dependent, and the inhibition of DNA repair, cell cycle redistribution, and apoptosis could be the mechanisms for the induction of radiosensitization by paclitaxel.

INTRODUCTION

Recent clinical research of new drug development has focused on a new chemotherapeutic agent: paclitaxel (TAX[3]), a diterpenoid plant product derived from the bark of the Western yew *Taxus brevifolia*, which has shown a broad activity in preclinical screening studies and a substantial activity against several refractory tumors in clinical setting (1, 2).

In vitro, this agent appears to have a mechanism of action by promoting microtubule assembly and stabilizing tubulin polymer formation (3) with consequent block in G_2-M phase of the cell cycle of proliferating, treated cells (4); its cytotoxicity is time-concentration dependent.

Radiosensitizer effect of TAX has been investigated extensively on the rationale that G_2+M is the most radiosensitive phase of the cell cycle (5, 6). In most of these combination studies, a significant radiation potentiating effect of TAX was found only after a TAX given dose that produced both a block in G_2-M phase and also a high cell killing (≅90%); in the clinical setting, this could result in damage to normal tissue. Moreover, literature data are contradictory; the combination of prolonged drug exposure (24 h) and XRT resulted in additive, supraadditive, or antagonistic interactions in a wide type of cell lines; the presence of arrest in G_2-M did not seem to be a sufficient condition to enhance radiation sensitivity (7, 8). Other mechanisms of TAX-XRT interaction could provide for a synergistic effect.

Therefore, recent works (9, 10) investigated new combination schedules with low TAX doses (subtherapeutic doses) that did not result in cell cycle perturbation to obtain information on: (*a*) the best synergistic effect as a result of the optimal combination of cell line characteristics, growth phase, drug concentration, and scheduling; and (*b*) the cellular mechanism of action involved for TAX-mediated radiosensitization as cytokinetic alterations, interference with postirradiation DNA repair, apoptosis, and reoxygenation (11, 12).

The aim of this study was to test different combinations of chemotherapeutic schedules and radiotherapy fractionated to obtain additional information of possible usefulness in the clinical setting.

Received 12/21/98; revised 4/14/99; accepted 4/19/99.

The costs of publication of this article were defrayed in part by the payment of page charges. This article must therefore be hereby marked *advertisement* in accordance with 18 U.S.C. Section 1734 solely to indicate this fact.

[1] This work was supported by a grant from Istituto Oncologicalo Romagnolo, Forlì, Italy.

[2] To whom requests for reprints should be addressed, at Department of Oncology, S. Maria delle Croci Hospital, Viale Randi 5, 48100, Ravenna, Italy. Phone: 39-544-285247; Fax: 39-544-285330; E-mail: marangolo@ra.nettuno.it.

[3] The abbreviations used are: TAX, Taxol (paclitaxel); XRT, X-ray treatment; IC_{50}, 50% inhibiting concentration; MID, mean inactivation dose; SER, sensitizer enhancement ratio; PI, propidium iodide; BrdUrd, 5-bromo-2′-deoxyuridine; SF, surviving fraction.

Table 1 Survival of HT29 and LoVo cells exposed to different TAX concentrations for various times
Culture medium with TAX was changed after 48 h. Values expressed are percentages of total cells.

Exposure to TAX (h)	HT29								LoVo							
	TAX doses (nM)							IC_{50} (nM)	TAX doses (nM)							IC_{50} (nM)
	0.5	1	5	10	50	100	1,000		1	5	10	50	100	1,000	10,000	
24	100[a]	95	69	51	28	7	7	10	100	100	97	67	58	39	6	400
48	100	91	75	63	22	6	3	20	87	61	46	41	35	5	9	8
72	100	100	95	71	21	8	0	25	91	73	53	48	37	3	5	34
96	100	100	100	78	4	5	0	15	100	97	73	65	42	2	2	80
120	100	100	100	80	0	0	0	14	100	100	82	70	48	2	0	96

[a] Data represent mean values from three separate experiments; SD <5%.

MATERIALS AND METHODS

Drugs and XRT

TAX was kindly supplied by Bristol-Myers Squibb and was diluted in sterile DMSO to a stock concentration of 1 mg/ml. Working concentrations were diluted in Earle's balanced salt solution (Life Technologies, Inc., Merelbeke, Belgium) and prepared fresh from the frozen state just before use. Escalating doses ranging from 0.5 to 1,000 nM were used (0.5, 1, 5, 10, 50, 100, and 1,000) for HT29 cells and to 10,000 nM for LoVo cells. The IC_{50} was calculated for each time exposure. Each sample, with or without concomitant drug exposure, was irradiated in Petri dishes (1-cm thick) at room temperature (22–25°C), using an X-ray unit (Philips: 200 kV, 20 mA, 0.1 mm Cu filter- XK 2600/00) at a dose rate of 0.6 Gy/min. Three schedules of combined TAX-XRT treatment were assayed in HT29 and LoVo cell lines:

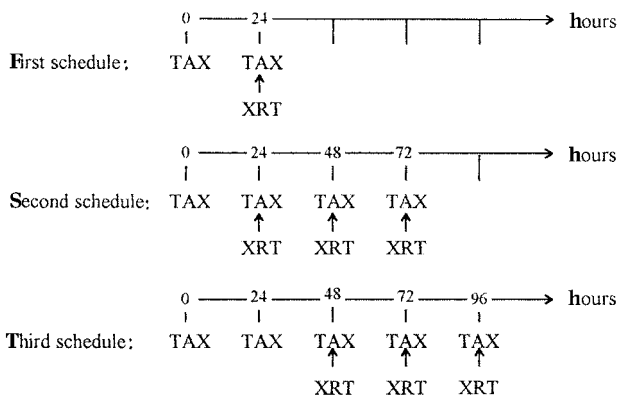

Cell Culture

The human colon adenocarcinoma cell lines, HT29 and LoVo, were provided by Dr. G. Zupi (Laboratory of Experimental Chemotherapy, Regina Elena Institute for Cancer Research, Rome, Italy). HT29 cells were grown in RPMI 1640 supplemented with 10% FCS, 1% L-glutamine, and 0.1% antibiotics; HT29 grew with doubling time of about 19 h. LoVo cells were grown in Nutrient Mixture F-12 with 15% FCS, 1% MEM, bicarbonate, sodium hydroxide, and 0.1% antibiotics; LoVo grew with doubling time of about 30 h. HT29 and LoVo cells were routinely subcultured using a 5-min exposure to Trypsin-EDTA solution and grown at 37°C in a humidified 5% CO_2/95% air atmosphere. All products for cell culture were from Life Technologies, Inc.

Clonogenic Assay

According to the most used and confirmed methods (13), for all experiments stock cultures were washed with EBSS, trypsinized, rinsed, and plated into 60-mm Petri dishes and incubated in fresh medium for 3 days prior to experiments so that the treatment was conducted in the phase for exponential growth. After exposure, cells were washed, trypsinized, harvested as a single cell suspension, and counted with Coulter Counter Model ZM (Coulter Electronics Ltd., Luton Beds, United Kingdom). Known aliquots were dispensed into Petri dishes in triplicate, and colony-forming efficiency was determined from the plating of cells after an incubation period of 2 weeks. Colonies were stained with 2% methylene blue (Carlo Erba, Milano, Italy), and only colonies containing 50 or more cells were counted. Cloning efficiency of the untreated cells (control) was normalized to 100%, and the cloning efficiency of treated cells was expressed as a percentage of control survival.

Data Analysis

The amount of drug that reduces the proliferation of treated cells of 50% of that controls (IC_{50}) was deduced from a linear regression analysis of dose-response curves. To characterize the radiosensitivity of the cell line and the change in radiosensitivity after treatment with TAX, the MID was calculated. Radiation survival curves were fitted with either one of the linear-quadratic equations: $\ln S = -\alpha D - \beta D^2$ or $\ln(S/S_{TAX}) = -\alpha D - \beta D^2$, were D is the radiation dose, S is the colony survival relative to the plating efficiency, and S_{TAX} is the relative survival of unirradiated cells exposed to TAX. According to Fertil *et al.* (14), coefficient α and β were used to integrate the area under the curve using a 12-point Gaussian formula and to obtain the MID value. SER was calculated by dividing the dose of radiation required to kill 90% of control cells by the dose of radiation required to kill 90% of cells exposed to TAX. The additivity status was determined from the ratio of survival to combined treatment (S_{COMB}) relative to the product of survival to radiation (S_{XRT}) and drug alone (S_{TAX}). $S_{COMB}/S_{XRT}{\cdot}S_{TAX} > 1$ defines infraadditive interaction; $S_{COMB}/S_{XRT}{\cdot}S_{TAX} < 1$ indicates supraadditive interaction.

Table 2 Cell cycle phase distribution of HT29 cells after TAX chronic exposure

Cells were treated with various TAX concentrations and subjected to flow cytometric analysis after treatment as described in "Materials and Methods." Culture medium with TAX was changed after 48 h.

		Time (h)				
Treatment	%	24	48	72	96	120
	G_1	55[a]	66	75	66	72
Control	S	41	22	18	30	22
	G_2/M	4	12	7	4	6
	G_1	53	66	75	67	71
0.5 nM	S	42	21	19	27	21
	G_2/M	5	13	6	6	8
	G_1	48	64	62	65	70
1 nM	S	44	23	25	28	24
	G_2/M	8	13	13	7	6
	G_1	44	63	63	63	70
5 nM	S	40	22	24	27	20
	G_2/M	16	15	13	10	10
	G_1	48	63	69	73	71
10 nM	S	36	22	16	21	21
	G_2/M	16	15	15	6	8
	G_1	52	34	F[b]	52	F
50 nM	S	33	52	F	34	F
	G_2/M	15	14	15	14	15
	G_1	1	11	F	F	F
100 nM	S	4	19	F	F	F
	G_2/M	95	70	88	90	80

[a] Data represent mean values from three separate experiments; SD, <5%.
[b] F, cells or nuclei detected as damaged.

Table 3 Cell cycle phase distribution of LoVo cells after TAX chronic exposure

Cells were treated with various TAX concentrations and subjected to flow cytometric analysis after treatment as described in "Materials and Methods." Culture medium with TAX was changed after 48 h.

		Time (h)				
Treatment	%	24	48	72	96	120
	G_1	41[a]	59	51	63	68
Control	S	34	16	29	20	17
	G_2/M	25	25	20	17	15
	G_1	40	58	56	62	66
1 nM	S	35	17	24	19	18
	G_2/M	25	25	20	19	16
	G_1	40	55	55	61	66
5 nM	S	35	19	26	17	15
	G_2/M	25	26	19	22	19
	G_1	40	51	56	58	68
10 nM	S	34	22	30	20	12
	G_2/M	26	27	14	22	20
	G_1	38	49	51	53	65
50 nM	S	34	20	21	22	12
	G_2/M	28	31	28	25	23
	G_1	37	44	55	44	52
100 nM	S	30	21	23	25	20
	G_2/M	33	35	22	31	28
	G_1	21	18	10	9	9
1,000 nM	S	19	16	35	35	36
	G_2/M	60	66	55	56	55
	G_1	9	14	9	11	10
10,000 nM	S	8	15	11	8	5
	G_2/M	83	71	80	81	85

[a] Data represent mean values from three separate experiments; SD, <5%.

Flow Cytometry

DNA Analysis. Progression of HT29 and LoVo cells through the cell cycle was determined by flow cytometry. At the end of each treatment, the cells (at least duplicate samples for each point) were washed, harvested, pooled, and then counted. The cell suspension was centrifuged at 1000 rpm for 10 min and fixed with 50% acetone-methanol (1:4 v/v) and 50% PBS at 4°C for at least 1 h before flow cytometric analysis. Approximately 1×10^6 fixed cells were suspended in a volume of 800 μl containing 75 KU/ml RNase (Sigma Chemical Co., St. Louis, MO) and 50 μg/ml PI (Sigma) for 30 min at room temperature. The fluorescence emission of stained cells was measured using a Cytoron Absolute Ortho (Becton Dickinson, San Jose, CA). DNA-dye complex fluorescence was excited by an argon ion laser. Flow studies measured the number of cells *versus* DNA content and allowed for the determination of the fraction of cells in each phase of cell cycle.

BrdUrd Analysis. DNA synthesis was assessed by incorporation of BrdUrd (Sigma) and by flow cytometric analysis. Cells were incubated with BrdUrd (10 μM) before completion of treatment with TAX and/or XRT. At the end of the pulse labeling period, BrdUrd containing medium was aspirated, and the cells were washed twice with PBS; finally, fresh culture medium was added, and the cultures were further incubated at 37°C. At various intervals of time after BrdUrd labeling (post-labeling times, t = 0, 2, 4, 24, and 48 h) cultures were trypsinized to obtain a monocellular suspension, washed with PBS, and fixed with 70% ethanol. Cells were then washed and treated with HCl 4N for 30 min at 37°C. After washing, the pellets were resuspended in 1 ml of $Na_2B_4O_7$ (pH 8.5) for 5 min, washed, treated with PBS-Triton X-100 0.5% for 3 min, and incubated with anti-BrdUrd-FITC (Becton Dickinson) for 30 min at 37°C. Finally, the samples were washed twice and resuspended in 1 ml of PBS containing 5 μg/ml of PI and 5.5 μg/ml of RNase for 30 min at 37°C before flow cytometric analysis.

Detection of Apoptosis. Apoptotic cells were detected by flow cytometric analysis using a Cytoron Absolute Ortho. PI was excited using a 488-nm line of an argon ion laser; each sample was analyzed using a very low threshold on the forward scatter signal to include in the analysis all of the populations in the samples. Because relatively early during apoptosis cells detach from the surface of the culture flask and float in the medium, floating cells were added to the trypsinized ones and measured together. Apoptosis was determined by two different flow cytometric techniques using nonpermeabilized and permeabilized cells (15). In the first procedure, nonpermeabilized cells were supravitally exposed to PI to identify apoptotic cells from living and necrotic cells, even in those cases in which low molecular weight DNA fragments do not take place. PI supravital exposure leaded to a difference in apoptotic and nonapoptotic cells in the ability of excluding the nonvital dye due to a membrane alteration typical of the apoptotic cells; in the second method, permeabilized cells were exposed to PI to determine the hypodiploid peak (sub-G_1 peak). The cells were centrifuged at 1000 rpm for 5 min and then processed with two different

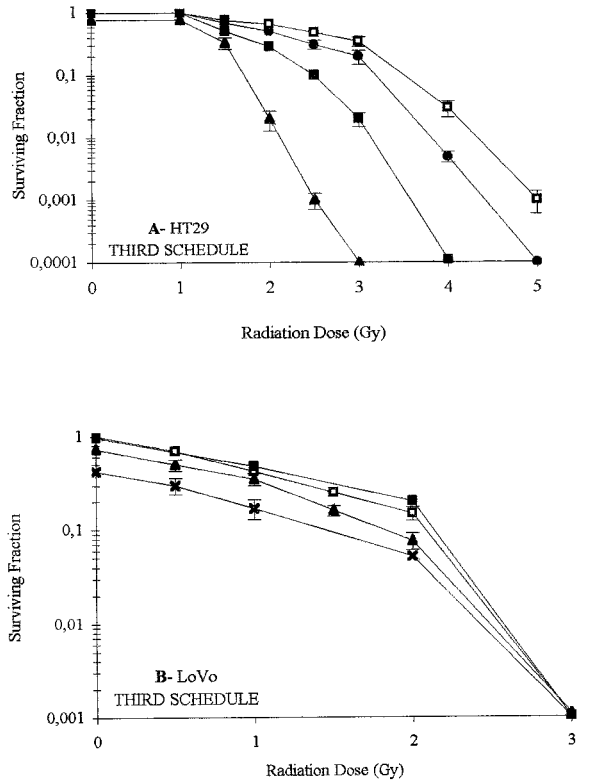

Fig. 1 Radiation survival curves with different TAX concentrations after third schedule administration. *A*, HT29 cells without (□; MID, 2.89 Gy) or with combined treatment with 1 nM (●; MID, 2.61 Gy), 5 nM (■; MID, 2.11 Gy), and 10 nM (▲; MID, 1.50 Gy) of TAX. SERs were approximately 1.1, 1.4, and 2.3 for 1, 5, and 10 nM, respectively. *B*, LoVo cells without (□; MID, 1.27 Gy) or with combined treatment with 5 nM (■; MID, 1.67 Gy), 10 nM (▲; MID, 1.16 Gy), and 100 nM (✕; MID, 1.15 Gy) of TAX. SERs were approximately 0.9, 1.2, and 1.5 for 5, 10, and 100 nM, respectively. Data were fitted to the linear quadratic equation given in "Materials and Methods." Culture medium was changed after 48 h. The effect of TAX alone on cell survival can be seen as the change in survival at 0 Gy. The results are given as the average of three experiments; *bars*, SD.

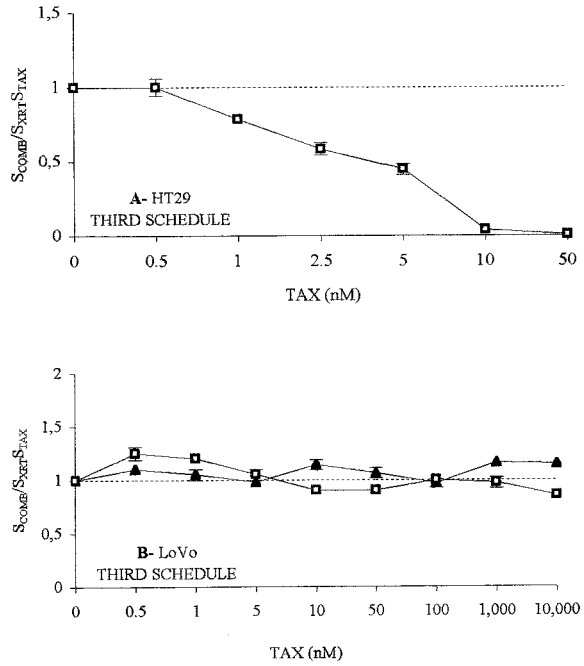

Fig. 2 Analysis of the outcome of the third schedule. *A*, HT29 cells (□, 2 Gy). SF for XRT alone was 65%. *B*, LoVo cells (▲, 1 Gy; □, 2 Gy). SF for XRT alone was 42 and 15% for 1 and 2 Gy, respectively. The additivity was determined as described in "Materials and Methods." The results are given as the average of three experiments; *bars*, SD.

methods: (*a*) nonpermeabilized cells (1×10^6) were resuspended in 0.5 ml PBS and then incubated with 1 ml of 40 μg/ml PI solution and 3 μg/ml RNase for 1.5 h at 37°C before the flow cytometric analysis. Apoptotic cells were detected on an forward scatter/PI dot plot as PI^{dim} peak; and (*b*) 1×10^6 cells were fixed in 2 ml of 70% cold ethanol at 4°C for 30 min. The cells were then centrifuged, washed twice in PBS, and resuspended in 0.5 ml PBS and 1 ml of hypotonic solution containing 40 μg/ml PI, and 3 μg/ml RNase. The mixed cells were incubated in the dark at room temperature for 10 min before the flow cytometric analysis. Analysis of DNA content was measured and displayed using a linear scale, which provided better assurance that objects with minimal DNA content are excluded from the analysis. Twenty thousand events/sample were acquired. As additional controls, a few samples were incubated with 0.1% sodium azide (Sigma), a substance that induces cell death through a nonapoptotic mechanism, and 100 nM dexamethasone (Sigma), a compound with apoptotic activity.

Analysis of p53, bcl-2, and bax Expression

For all experiments, cells were fixed and permeabilized using 0.25% paraformaldehyde in PBS (15 min at room temperature), followed by 70% cold methanol (60 min at 4°C). After washing in PBS, 1×10^6 cells were incubated (30 min at 4°C) with 10 μl of FITC-conjugated anti-p53 (clone DO-7; Dako, Milano, Italy) or FITC-conjugated anti-bcl-2 (clone 124; Dako); staining of bax was done with an indirect immunofluorescence method using a rabbit polyclonal IgG1 anti-bax protein (Dako) and a secondary antibody, anti-rabbit FITC conjugated. Negative controls were performed replacing anti-p53 and anti-bcl-2 with mouse IgG1 and anti-bax with rabbit IgG1. Moreover, MCF-7 and SK-BR3 cell lines were used as positive controls for bcl-2 staining and as negative and positive controls for p53 analysis, respectively. The fluorescence intensity of 10,000 cells stained with FITC was measured using a Cytoron Absolute Ortho.

Morphological Analysis of HT29 and LoVo Cells

For morphological assessment, attached and detached cells were counted and washed, and cytocentrifuge slides were prepared, air-dried, and stained by May Grünwald-Giemsa technique. Cell morphology was examined by light microscopy using a Zeiss Axiophot-2 microscope. Cell death was determined based on the expression of morphological features characteristic either of apoptosis (*e.g.*, cell shrinkage, nuclear condensation and fragmentation, extensive formation of membrane blebs, and apoptotic bodies) or of necrosis (*e.g.*, cell swelling, nuclear expansion, and gross cytolysis). The morphology of at

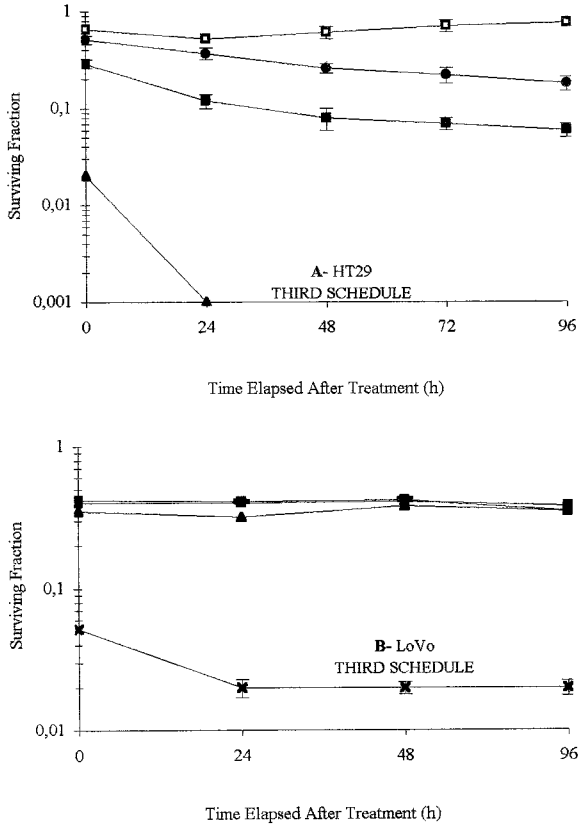

Fig. 3 Posttreatment evolution after third schedule administration. *A*, HT29 cells without (□, 2 Gy) or with combined treatment with 1 nM (●), 5 nM (■), and 10 nM (▲) of TAX. *B*, LoVo cells without (□, 2 Gy) or with combined treatment with 5 nM (■), 10 nM (▲), and 100 nM (✕) of TAX. The results are given as the average of three experiments; *bars*, SD.

Table 4 Analysis of the cell cycle redistribution of HT29 cells after the third schedule of TAX-XRT administration

Cells were exposed to third schedule of TAX-XRT treatment and subjected to flow cytometric analysis after treatment as described in "Materials and Methods." Culture medium with TAX was changed after 48 h.

	Hours after treatment				
Treatment	0	24	48	72	96
Control					
G_1	72[a]	63	73	80	91
S	19	25	16	17	6
G_2/M	9	12	11	3	3
1 nM TAX + 3 × 2 Gy					
G_1	50	38	37	56	61
S	32	44	46	30	28
G_2/M	18	18	17	14	11
5 nM TAX + 3 × 2 Gy					
G_1	43	34	35	57	59
S	38	48	40	31	30
G_2/M	19	18	25	12	11
10 nM TAX + 3 × 2 Gy					
G_1	43	30	47	49	50
S	41	57	38	39	38
G_2/M	16	13	15	12	12
3 × 2 Gy					
G_1	60	52	61	70	76
S	26	37	27	12	9
G_2/M	14	11	12	18	15

[a] From three separate experiments; SD, <5%.

least 500 cells was scored from each sample to determine the frequency of apoptotic death.

RESULTS

Effect of Chronic Exposure to TAX on Cell Survival and Cell Cycle Progression of HT29 and LoVo Cells. Cell survival was determined by a clonogenic assay. Table 1 shows the SF of exponentially growing HT29 cells as a function of different times of exposure (24–120 h) to escalating concentrations of TAX ranging from 0.5 to 1000 nM. Cells incubated with the same concentration of DMSO were not affected (data not shown). In HT29 cells, survival and cell cycle proliferation during 120 h of exposure (Tables 1 and 2) were not affected by the lowest TAX doses (0.5–1 nM); chronic exposure to 5 and 10 nM TAX induced a decline of cell survival and a moderate and temporary G_2-M block. The SF was 69% (5 nM) and 51% (10 nM) after 24 h and gradually recovered to 100 and 80%, respectively, after 120 h. The SF of HT29 cells was greatly reduced only with concentrations of TAX up to 50 nM at all times of exposure (Table 1). Cell cycle analysis at 50 nM TAX showed a broad peak in the lower channel numbers, indicating that cells had lost DNA and were damaged. After 72 h of 50 nM TAX incubation, this peak become more extensive (~80% of treated cells), including a portion of cells that overlapped the channels for cells with G_1-S-phase content (Table 2). Concentrations of drug up to 50 nM also resulted in a stable G_2-M block (at all times of incubation). Recovery studies did not show repair of drug damage and cycling out of G_2-M block at these high doses (data not show).

The response of LoVo cells to chronic TAX exposure (Table 1) were similar to that of HT29 cells, but LoVo cells were at least 40 times less sensitive after 24 h of TAX exposure; in fact, the mean IC_{50} was in the range of 10 nM for HT29 cells and 400 nM for LoVo cells. In contrast to the HT29 cells, LoVo cells showed a great enhanced cell killing only after 48 h of TAX exposure (IC_{50} = 20 nM and IC_{50} = 8 nM for HT29 and LoVo, respectively). The difference in sensitivity may be due to different doubling times of the two cell lines (19 and 30 h for HT29 and LoVo cells, respectively). After 72 h of TAX exposure, an increase in LoVo cell survival with 1–100 nM TAX was also noticed. Table 3 shows the effect of chronic exposure (24–120 h) to different TAX concentrations on cell cycle distribution of LoVo cells. Below 50 nM TAX, the phase fraction of treated cells did not differ significantly from the control; concentrations up to 50 nM TAX resulted in the characteristic G_2-M block at all tested times without production of the nuclear damage found in HT29.

HT29 and LoVo Cell Survival in Combined Treatment with TAX and XRT. The first schedule was predominantly additive in HT29 cells and additive or infraadditive in LoVo cells. Flow cytometric analysis did not show perturbation of cells cycle progression in both HT29 and LoVo cells (data not shown).

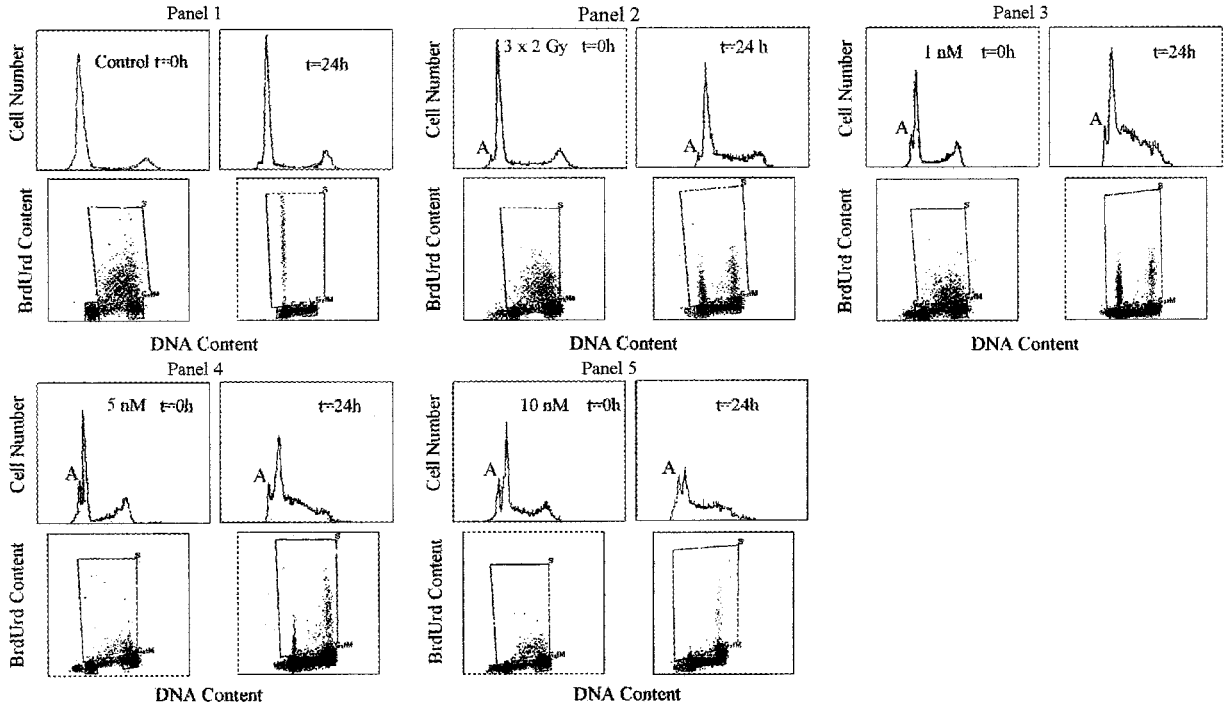

Fig. 4 Flow cytometric detection of DNA content, apoptotic cells, and BrdUrd incorporation in HT29 cells. Analysis was performed at the end of the third schedule or TAX-XRT combination (t = 0 h) and after 24 h postrecovery (t = 24 h). *Panel 1,* control cells; *Panel 2,* XRT alone (3 × 2 Gy); *Panels 3–5,* cells exposed to the third schedule with 1, 5, and 10 nM TAX, respectively. *A,* sub-G_1 apoptotic peak. Data were obtained from bivariate flow cytometric analysis on DNA fluorescence (PI) or immunofluorescence (BrdUrd). Linear scale was used for analysis of DNA content in fixed cells.

In the second schedule, the TAX-XRT interaction was additive and infraadditive in HT29 and LoVo cells, respectively. No alteration of cell cycle distribution was found (data not shown).

In the third schedule, the effect of combined treatment was first investigated as a function of the XRT dose using fixed drug doses. TAX doses below the IC_{50} value were able to increase radiosensitivity of HT29 cells at radiation doses starting from 2 Gy (Fig. 1*A*). The rate of radiosensitization was dependent on the concentration of TAX, with the highest decrease in MID value at 10 nM TAX: MID = 2.89 Gy for 3 × 2 Gy alone (combination of three treatment days with 2 Gy XRT) and MID = 1.5 Gy for 10 nM TAX and three times 2 Gy; maximal SER was 2.3 with 10 nM TAX. In contrast in LoVo cells, the TAX-XRT interaction produced a profile similar to that determined for XRT alone (Fig. 1*B*), and no significant decrease of MID values was found.

The drug concentration dependence of HT29 and LoVo cell survival with concomitant exposure to radiation is shown in Fig. 2. The dose radiation of 2 Gy was chosen because it represents a clinically relevant radiotherapeutic dose. In HT29 cells, the combination of 3 × 2 Gy in continuous presence of TAX was supraadditive and dose dependent over 0.5 nM TAX. Moreover, posttreatment recovery study showed a loss of cell survival and the inability to overcome the damage in the following 96 h after the end of treatment (Fig. 3*A*). These survival data correlated with alteration produced on cell cycle progression compared with control (Table 4). In fact, at the end of treatment, most of the HT29 cells were accumulated overall in S phase, S-G_2 junction, and to a smaller extent in the G_2-M phase with concomitant depletion of the G_1 compartments. This figure persisted after 96 h of posttreatment recovery, indicating that progression through the cell cycle was delayed (1–5 nM TAX) or blocked (10 nM).

Bivariate flow cytometric analysis of the cell cycle progression using pulse-chose BrdUrd labeling showed that at the end of treatment, BrdUrd-positive HT29 cells were decreased in treated cells with respect to control (Fig. 4). Treated BrdUrd-positive cells demonstrated an initial delay at the S-G_2 junction, and after 24 h of pulse labeling, the G_2-M block and the small G_1 repopulation suggest that only a few BrdUrd-positive cells could progress through the block. The duration of the G_2-M delay is related to the level of unrepaired damage present in the cells as they approach mitosis (16). Moreover, after treatment, there was a percentage of BrdUrd-negative HT29 cells in S phase that was not able to progress in the following recovery day. Twenty-four h after the pulse labeling, BrdUrd-negative cells initially in the G_1 compartment had time to reach this S phase block, but while the cohort of control BrdUrd-negative HT29 cells progressed into the following G_1 phase, treated BrdUrd-negative cells remained blocked in S and G_2-M phase after 96 h of recovery (data not shown). In HT29 cells, the third schedule seems to produce the inability to overcome DNA damage, as shown by impaired postrecovery; stabilization of the

Table 5 Analysis of the cell cycle redistribution of LoVo cells after the third schedule of TAX-XRT administration

Cells were exposed to the third schedule of TAX-XRT treatment and subjected to flow cytometric analysis as described in "Materials and Methods." Culture medium with TAX was changed after 48 h.

	Hours after treatment			
Treatment	0	24	48	72
Control				
G_1	63[a]	65	69	75
S	20	13	7	10
G_2/M	17	22	24	15
5 nM TAX + 3 × 1 Gy				
G_1	64	62	71	76
S	19	14	8	9
G_2/M	17	24	21	15
10 nM TAX + 3 × 1 Gy				
G_1	66	66	69	75
S	20	13	8	10
G_2/M	14	21	23	15
50 nM TAX + 3 × 1 Gy				
G_1	65	61	68	74
S	20	14	9	8
G_2/M	15	25	23	18
3 × 1 Gy				
G_1	67	61	69	73
S	19	13	6	8
G_2/M	14	26	25	19
10 nM TAX + 3 × 2 Gy				
G_1	61	63	60	48
S	16	15	19	26
G_2/M	23	22	21	26
50 nM TAX + 3 × 2 Gy				
G_1	58	60	56	49
S	17	15	20	27
G_2/M	25	25	24	24
3 × 2 Gy				
G_1	60	63	61	65
S	15	15	20	13
G_2/M	25	22	19	22

[a] Data represent mean values from three separate experiments; SD, <5%.

microtubule dynamics and radiation repair could be interrelated. In HT29 cells, treatment with XRT alone (3 × 2 Gy; SF, 65%) induced a smaller accumulation of tumor cells into S and G_2-M in comparison to the TAX-XRT combination. The HT29 cells were able to progress through the block and replenished the G_1 compartment. In fact, after 24 h of pulse labeling, BrdUrd-positive cells (Fig. 4) were delayed with respect to control but also were able to progress into the following G_1 phase after 48 h of recovery (data not shown).

Fig. 2*B* shows the effect of drug concentration on fixed radiation doses of 1–2 Gy in LoVo cells. Because of the great reduction of SF obtained with 3 × 2 Gy (SF, 15%), we also chose for combination experiments with the 1-Gy doses (SF, 42%). A weak supradditive interaction was showed only in the presence of 10–50 nM TAX and 3 × 2 Gy; at these doses, the progression through the cell cycle was arrested and was only resolved after 72 h of posttreatment recovery. Interaction between TAX and 3 × 1 Gy was weakly additive and did not produce alteration of cell cycle progression respect to controls (Table 5). Analysis of post-XRT recovery did not produce an appreciable variation of cytotoxicity for up to 96 h (Fig. 3*B*).

Identification of Apoptotic Cells. Apoptosis is the major mechanism by which ionizing radiation and most chemotherapeutic agents cause tumor cell death (17). By flow cytometric analysis of DNA content, apoptotic cells were quantitatively evaluated by two different methods (see "Materials and Methods").

Fig. 4 and Table 6 illustrate sub-G_1 apoptotic HT29 peak. Very few spontaneous apoptotic HT29 cells were detected in the control (0.6%). After treatment with 3 × 2 Gy alone, the number of apoptotic cells represent 5% of the total cell number. Treatment with TAX alone induced apoptosis only after 24 h of drug-free medium: 0.6% (1 nM), 2% (5 nM), and 8% (10 nM). Higher doses of TAX treatment resulted in DNA fragmentation and G_2-M arrest but not in apoptosis. The number of apoptotic HT29 cells detected, following the third schedule of combination, was increased with respect to control and strictly dependent on the TAX concentrations: 9% (1 nM), 13% (5 nM), and 22% (10 nM) at the end of treatment and 6% (1 nM), 8% (5 nM), and 15% (10 nM) after 24 h of drug-free medium. HT29 incubation with sodium azide markedly enhanced the number of dead cells but did not produce evidence of apoptotic cells (0%), whereas dexamethasone induced only a small percentage of apoptotic cells (8%). Similar percentages of apoptotic cells (Table 6) were obtained by analysis of supravital exposure to PI, which was able to give quantitative information about apoptotic cell populations and necrotic cells. No evidence of apoptotic cell death was obtained in LoVo cells (data not shown).

Morphological criteria of identification of apoptotic and necrotic cells were taken into consideration in conjunction with flow cytometric analysis. Microscopic examination of treated HT29 cells (Fig. 5) revealed changes in cell morphology typically seen in cells undergoing apoptosis as cell shrinkage, nuclear condensation, and fragmentation. In particular, HT29 cells treated with 10 nM TAX and 3 × 2 Gy also exhibited formation of "apoptotic bodies," rupture of the apoptotic cells into debris, and morphology suggestive of necrosis. In contrast, morphological features characteristic of apoptosis were not observed in LoVo cells (data not shown).

Flow Cytometric Analysis of p53, bcl-2, and bax Expression. It has long been recognized that apoptotic cell death can be controlled by various stimuli acting as promoters (*e.g.*, bax, Fas, and p53), effectors (interleukin 1β converting enzyme-like protease), or inhibitors (*e.g.*, bcl-2, Mcl-1, and Bcl-XL; Ref. 18). The expression of apoptosis-associated proteins p53, bcl-2, and bax were detected by flow cytometry in both cell lines. With the p53 antibody DO-7, HT29 and LoVo cells were positive and negative, respectively (Table 7). The treated LoVo cells showed an increased of positive p53 (~30%). After treatments, in HT29 cells no changes in the expression of p53 were observed. This suggests that a p53-independent pathway could be involved in the apoptotic process. bax and bcl-2 proteins are able to form homo- and heterodimers; therefore, it has been proposed that the relative sensitivity of cells to apoptotic stimuli is dependent on the bax:bcl-2 ratio (19, 20). HT29 cells inherently expressed a higher bax:bcl-2 ratio than LoVo cells. This could have contributed to the differences in sensitivity to undergo apoptosis. Moreover, the TAX treatments were able to weakly decrease the expression of antiapoptotic bcl-2 protein in HT29 cells.

Table 6 Percentage of apoptotic HT29 cells after third schedule administration as identified by three different techniques

Treatment	Sub-G_1 peak		PI supravital exposure		Morphology	
	0 h	24 h[a]	0 h	24 h	0 h	24 h
Control	0.6[b]	0.6	1	1	1.6	1
1 nM TAX	0	0.6	0	1	ND[c]	ND
5 nM TAX	0	2	0	2	ND	ND
10 nM TAX	0	8	0	10	ND	5
3 × 2 Gy	5	5	7	6	3	3
1 nM + 3 × 2 Gy	9	6	11	6	ND	ND
5 nM + 3 × 2 Gy	13	8	12	7	ND	ND
10 nM + 3 × 2 Gy	22	15	20	10	15	8
Sodium azide, 0.1%	0	0	0	0	0	0
Dexamethasone, 100 nM	8	ND	7	ND	6	ND

[a] 24 h drug-free medium.
[b] Data represent mean values from three separate experiments; SD, <5%.
[c] ND, not determined.

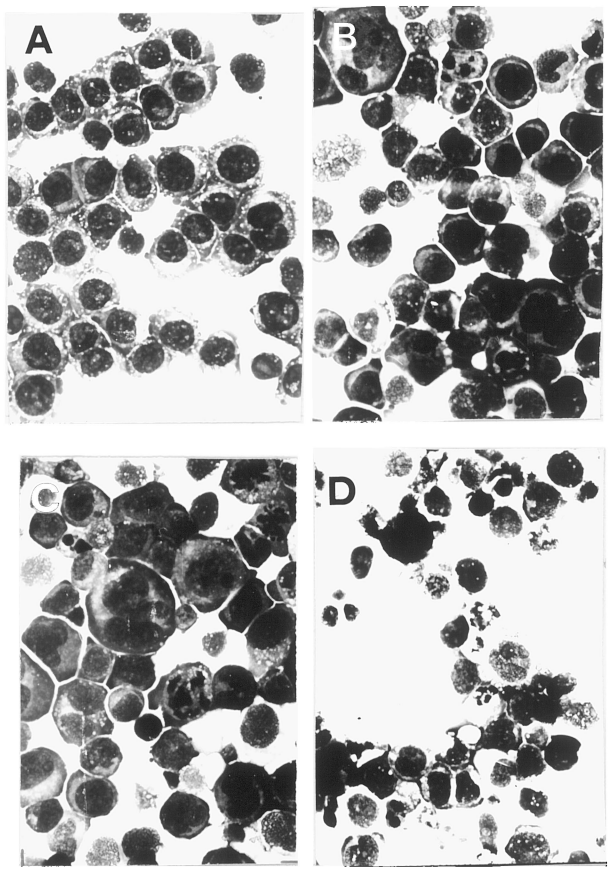

Fig. 5 Morphological appearance of HT29 cells treated with the third schedule of combination. *A*, cells without treatment. *B–D*, 10 nM TAX + 3 × 2 Gy. The cells were stained with May Grünwald-Giemsa as described in "Materials and Methods." Treatment induced apoptotic changes such as cell shrinkage, chromatin condensation, nuclear fragmentation, and "apoptotic bodies." ×500.

Table 7 Percentage of p53, bcl-2, and bax proteins by flow cytometry in HT29 and LoVo cells

Cells were exposed to different TAX-XRT administrations and subjected to flow cytometric analysis as described in "Materials and Methods."

Cell lines	p53	bcl-2	bax
HT29			
Control at 4 days of growth	80[a]	84	89
Control at 7 days of growth	83	86	87
3 × 2 Gy	85	89	88
10 nM TAX for 2 days	82	76	86
10 nM TAX for 4 days	83	75	93
10 nM TAX + 3 × 2 Gy	81	74	98
LoVo			
Control at 4 days of growth	2	96	54
Control at 7 days of growth	2	98	57
3 × 2 Gy	37	97	63
10 nM TAX for 2 days	30	95	60
10 nM TAX for 4 days	33	94	58
10 nM TAX + 3 × 2 Gy	28	91	61

[a] Data represent mean values from three separate experiments; SD, <5%.

DISCUSSION

The interaction between radiation and chemotherapy may be roughly divided into four generic types: (*a*) spatial cooperation in which each modality treats different anatomical site; (*b*) toxicity independence in which the respective toxicities are not overlapping; (*c*) radioprotection in which normal tissues are protected by noncytotoxic agents; and (*d*) enhancement of tumor response in which the interaction may be additive, infraadditive, or supraadditive. The *in vitro* role of TAX as radiosensitizer was widely studied. The obtained results were contradictory and depended on cell lines, drug concentration, and time scheduling of TAX-XRT.

The TAX-XRT interaction was found supraadditive in human astrocytoma (5), breast (6), pancreas (8), ovarian (9, 10), cervical (9, 21, 22), leukemia (23), lung (24), prostate (25), and head and neck (21, 26) carcinoma cell lines and glioma cell lines (27). Other studies have not reported any radiosensitization effect in lung carcinoma (6), colon (28), and cervix cell lines (29). Moreover, some reports showed contradictory results in the same cell line as in prostatic (25, 28), breast (6, 28), and cervical squamous carcinoma (9, 30).

However, on the basis of the above studies (5, 9, 28, 30), it seems that the presence of the G_2-M block may not be the

main condition for a synergistic interaction between TAX and XRT, but more than one mechanisms may act as TAX concentration, exposure time, time scheduling of drug and XRT, interference with postirradiation DNA repair, p53 expression, apoptosis, and cell line type (9, 10, 19). Moreover, it seems important to obtain a radiosensitization effect to: (*a*) perform an accurate timing and duration of TAX treatment to allow the use of low TAX concentrations, which did not result in cell cycle perturbations and toxicity; and (*b*) find the optimal time scheduling of TAX and XRT.

This study investigated the optimal sequence of combination in two human colon adenocarcinoma cell lines (HT29 and LoVo) and was based on previous works indicating that TAX pretreatment at 48 h prior to XRT (9, 10) and/or chronic exposure of low TAX concentration in combination with fractionated irradiations led to a higher radiosensitizing effect (24).

The induction of radiosensitization by TAX was shown to be strongly schedule dependent. In HT29 cells, the first and second schedules resulted in an additive effect, whereas a supraadditive interaction was detected with the third schedule; this effect was obtained with amounts of TAX lower than IC_{50} and was dose dependent.

In LoVo cells, TAX showed a weak radiosensitization effect. The first and second schedules of combination were infraadditive, whereas the third schedule was additive. Also, an additive interaction between drug and XRT can be considered a good radiosensitization (26). The interaction between XRT and TAX in LoVo cells was dependent on XRT dose but not on TAX concentration, and the additive effect was obtained with XRT dose with a high cell killing and an amount of drug in the range of IC_{50}. HT29 and LoVo cells showed a different sensitivity to drug alone and to radiation alone.

HT29 cells were more sensitive to TAX exposure than LoVo cells. Differential sensitivity was dependent on time of exposure to the drug and was, probably, due to a different proliferation rate; a similar IC_{50} was obtained after 24 h of TAX treatment in HT29 cells (10 nM; doubling time, 19 h) and after 48 h in LoVo cells (8 nM; doubling time, 30 h).

LoVo cells (MID, 1.27 Gy) appeared more radiosensitive than HT29 cells (MID, 2.89 Gy) and showed a different cell cycle redistribution after XRT exposure. Loss of cellular ability to repair DNA damage and other biochemical and molecular processes can be considered main factors in enhancing radiosensitivity. In contrast to LoVo cells, a wide shoulder characterized the HT29 radiation survival curve, which reflects the accumulation and repair of sublethal lesions. In fact, post-XRT recovery studies of the cytotoxicity showed an enhancement of survival in HT29 cells and an inability to overcome the damage in LoVo cells.

The supraadditive interaction in HT29 cells was obtained with amounts of TAX lower than IC_{50}, which do not result in cell cycle perturbation. These data suggest that a G_2-M block is not a condition for TAX to act as radiosensitizer, and more than one mechanism are involved in determining a supraadditive response (9, 10, 26). In fact, the third schedule of combination resulted in a perturbation of cell cycle distribution in an effective impairment of cellular ability in repairing DNA damage and in apoptotic cell death in HT29 cells but not in LoVo cells. Cell cycle distribution (31, 32) and inhibition of postirradiation DNA damage repair (33, 34) are likely to result in supraadditive radiation-drug interaction. The characteristic suppression of the XRT survival curve shoulder in HT29 cells (Fig. 1*B*) is likely to proceed from these cooperative effects. Indeed, in LoVo cells, these mechanisms do not share a common pathway, and repair interaction and cytokinetic cooperation appear not to be involved in the combination.

HT29 cells have high constitutional expression levels of p53. LoVo cells are p53 negative, and its expression is induced by treatments. Safran *et al.* (35) suggest that the response to TAX plus concurrent XRT do not seem to be p53 dependent, and a p53-independent pathway could be activated overall during the combination treatment. The bax:bcl-2 ratio was evaluated in both cell lines; HT29 cells showed a lower ratio than LoVo cells, the value of which is decreased by combined treatment; this could explain the constitutional inability of the LoVo cells to undergo apoptosis. However, HT29 seems to have a low propensity to undergo apoptosis; the absence of p53 wild-type and the bcl-2-positive expression can raise the threshold for apoptosis induction directly or by interfering with the expression of other regulatory apoptotic genes (36, 37).

Our data suggest that the choice of an appropriate time scheduling of drug and radiation permit the use TAX concentrations and radiation doses that may be given in a clinical setting. The radiation-enhancing effect of low TAX doses can be explained by more than one interaction mechanism as the interference with postradiation DNA repair, an impaired cell cycle progression, and apoptosis.

The results of these experiments have great impact on the clinical setting; the treatment of local and/or regional relapses of colorectal cancer is a combination of chemo- and radiotherapy, chiefly in nonpretreated patients. The main clinical goal is to induce tumor shrinkage and to render bulky tumors operable at the time of relapse so that more active radiotherapy is needed with higher cost-benefit for the patients.

If these preclinical data are confirmed in a clinical setting, a realistic benefit for patients will be achieved: a reduction of time exposure to radiation therapy, 3 days of 5 for each week of treatment, a maintenance of the same tumor response with lower radiation dose, and probably reduced toxic local and systemic side effects, which will be able to increase the therapeutic index of a treatment with palliative or radical intent.

ACKNOWLEDGMENTS

We thank Dr. G. Zupi of Laboratory of Experimental Chemotherapy, Regina Elena Institute for Cancer Research, Rome, for scientific and technical assistance.

REFERENCES

1. Liebmann, J. E., Cook, J. A., Lipschultz, C., Teague, D., Fisher, J., and Mitchell, J. B. Cytotoxic studies of paclitaxel (Taxol) in human tumor cell lines. Br. J. Cancer, *68:* 1104–1109, 1993.

2. Rowinsky, E. K., Cazenave, C. A., and Donehower, R. C. Taxol: a novel investigational antimicrotubule agent. J. Natl. Cancer Inst., *82:* 1247–1259, 1990.

3. Schiff, P. B., Fant, J., and Horwitz, S. B. Promotion of microtubule assembly *in vitro* by Taxol. Nature (Lond.), *277:* 665–667, 1979.

4. Schiff, P. B., and Horwitz, S. B. Taxol stabilizes microtubules in mouse fibroblast cells. Proc. Natl. Acad. Sci. USA, *77:* 1561–1565, 1980.

5. Tishler, R. B., Schiff, P. B., Geard, C. R., and Hall, E. J. Taxol: a novel radiation sensitizer. Int. J. Radiat. Oncol. Biol. Phys., *22:* 613–617, 1992.

6. Liebmann, J., Cook, J. A., Fisher, J., Teague, D., and Mitchell, J. B. Changes in radiation survival curve parameters in human tumor and rodent cells exposed to paclitaxel (Taxol). Int. J. Radiat. Oncol. Biol. Phys., *29:* 559–564, 1994.

7. Hei, T. K., and Hall, E. J. Taxol, radiation, and oncogenic transformation. Cancer Res., *53:* 1368–1372, 1993.

8. Liebmann, J., Cook, J. A., Fisher, J., Teague, D., and Mitchell, J. B. *In vitro* studies of Taxol as a radiation sensitizer in human tumor cells. J. Natl. Cancer Inst., *86:* 441–446, 1994.

9. Steren, A., Sevin, B. U., Perras, J., Ramos, R., Angioli, R., Nguyen, H. N., Koechli, O. R., and Averette, H. E. Taxol as a radiation sensitizer: a flow cytometric study. Gynecol. Oncol., *50:* 89–93, 1993.

10. Rodriguez, M., Sevin, B. U., Perras, J., Nguyen, H. N., Pham, C., Steren, A. J., Koechli, O. R., and Averette, H. E. Paclitaxel: a radiation sensitizer of human cervical cancer cells. Gynecol. Oncol., *57:* 165–169, 1995.

11. Milas, L., Hunter, N. R., Mason, K. A., Milross, C. G., and Peters, L. J. Tumor reoxygenation as a mechanism of taxol-induced enhancement of tumor radioresponse. Acta Oncol., *34:* 409–412, 1995.

12. Milas, L., Hunter, N. R., Mason, K. A., Milross, C. G., Saito, Y., and Peters, L. J. Role of reoxygenation in induction of enhancement of tumor radioresponse by paclitaxel. Cancer Res., *55:* 3564–3568, 1995.

13. Zupi, G., Marangolo, M., Arancia, G., Greco, C., Laudonio, N., Iosi, F., Formisano, G., and Malorni, W. Modulation of the cytotoxic effect of 5-fluorouracil by *N*-methylformamide on a human colon carcinoma cell lines. Cancer Res., *48:* 6193–6200, 1988.

14. Fertil, B., Dertinger, H., Courdi, A., and Malaise, E. P. Mean inactivation dose: a useful concept for intercomparison of human cell survival curves. Radiat. Res., *99:* 73–84, 1984.

15. Zamai, L., Falcieri, E., Marhefka, G., and Vitale, M. Supravital exposure to propidium iodide identifies apoptotic cells in the absence of nucleosomal DNA fragmentation. Cytometry, *23:* 303–311, 1996.

16. Nagasawa, H., Keng, P., Harley, R., Dahlberg, W., and Little, J. B. Relationship between γ-ray-induced G_2/M delay and cellular radiosensitivity. Int. J. Radiat. Biol., *66:* 373–379, 1994.

17. Kerr, J. F. R., Winterford, C. M., and Harmon, B. V. Apoptosis. Its significance in cancer and cancer therapy. Cancer (Phila.), *73:* 2013–2026, 1994.

18. Gorman, A. M., Samali, A., McGowan, A. J., and Cotter, T. G. Use of flow cytometry techniques in studying mechanisms of apoptosis in leukemic cells. Cytometry, *29:* 97–105, 1997.

19. Oltvai, Z., Milliman, C., and Korsmeyer, S. J. Bcl-2 heterodimerizes *in vivo* with a conserved homolog, Bax, that accelerates programmed cell death. Cell, *74:* 609–619, 1993.

20. Chresta, C. M., Masters, J. R. W., and Hickman, J. A. Hypersensitivity of human testicular tumors to etoposide-induced apoptosis is associated with functional p53 and a high Bax:Bcl-2 ratio. Cancer Res., *56:* 1834–1841, 1996.

21. Hennequin, C., Giocanti, N., and Favaudon, V. Interaction of ionizing radiation with paclitaxel (Taxol) and docetaxel (Taxotere) in HeLa and SQ20B cells. Cancer Res., *56:* 1842–1850, 1996.

22. Chi, K. H., Chow, K. C., and Chen, K. Y. Optimal combination of Taxol with radiotherapy. Proc. Am. Assoc. Cancer Res., *36:* 612, 1995.

23. Choy, H., Rodriguez, F. F., Koester, S., Hilsenbeck, S., and Von Hoff, D. D. Investigation of Taxol as a potential radiation sensitizer. Cancer (Phila.), *71:* 3774–3778, 1993.

24. Van Rijn, J., Van der Berg, J., and Meijer, O. W. M. Proliferation and clonal survival of human lung cancer cells treated with fractionated irradiation in combination with paclitaxel. Int. J. Radiat. Oncol. Biol. Phys., *33:* 635–639, 1995.

25. Lokeshwar, B. L., Ferrell, S. M., and Block, N. L. Enhancement of radiation response of prostatic carcinoma by Taxol: therapeutic potential for late-stage malignancy. Anticancer Res., *15:* 93–98, 1995.

26. Leonard, C. E., Chan, D. C., Chou, T. C., Kumar, R., and Bunn, P. A. Paclitaxel enhances *in vitro* radiosensitivity of squamous carcinoma cell lines of the head and neck. Cancer Res., *56:* 5198–5204, 1996.

27. Gupta, N., Hu, L., Fan, P. D., and Deen, D. F. Effect of Taxol and radiation on brain tumor cell lines. Proc. Am. Assoc. Cancer Res., *35:* 647, 1994.

28. Stromberg, J. S., Lee, Y. J., Armour, E. P., Martinez, A. A., and Corry, P. M. Lack of radiosensitization after paclitaxel treatment of three human carcinoma cell lines. Cancer (Phila.), *75:* 2262–2268, 1995.

29. Minarik, L., and Hall, E. J. Taxol in combination with acute and low dose rate irradiation. Radiother. Oncol., *32:* 124–128, 1994.

30. Erlich, E., McCall, A. R., Potkul, R. K., Walter, S., and Vaughan, A. Paclitaxel is only a weak radiosensitizer of human cervical carcinoma cell lines. Gynecol. Oncol., *60:* 251–254, 1996.

31. Jonh, M., Flam, M., Legha, S., and Phillips, T. (eds.). Chemoradiation: An Integrated Approach to Cancer Treatment, Ed. 1. Philadelphia, J. B. Lippincott Co., 1995.

32. McGinn, C. J., Shenwach D. S., and Lawrence, T. S. Radiosensitizing nucleotides. J. Natl. Cancer Inst., *88:* 1193–1203, 1996.

33. Ward, J. F. Mechanism of DNA repair and their potential modification for radiotherapy. J. Radiat. Oncol. Biol. Phys., *12:* 1027–1032, 1986.

34. Giocanti, N., Hennequin, C., Balosso, J., Mahler, M., and Favaudon, V. DNA repair and cell cycle interaction in radiation sensitization by the topoisomerase II poison etoposide. Cancer Res., *53:* 2105–2111, 1993.

35. Safran, H., King, T., Choy, H., Gollerkeri, A., Kwakwa, H., Lopez, F., Cole, B., Myes, J., Tarpey, J., and Rosmarin, A. p53 mutations do not predict response to paclitaxel/radiation for nonsmall cell lung carcinoma. Cancer (Phila.), *78:* 1203–1210, 1996.

36. Fisher, D. E. Apoptosis in cancer therapy: crossing the threshold. Cell, *78:* 539–542, 1994.

37. Miyashita, T., and Reed, J. C. Tumor suppressor p53 is a direct transcriptional activator of human *bax* gene. Cell, *80:* 293–299, 1995.

Clinical Cancer Research

Paclitaxel and Radiotherapy: Sequence-dependent Efficacy—A Preclinical Model

Alessandra Niero, Ermanno Emiliani, Giuseppe Monti, et al.

Clin Cancer Res 1999;5:2213-2222.